MAGNETO-ACOUSTIC OSCILLATOR

Tanay A. Gosavi[1] *and Sunil A. Bhave*[2]
[1]Cornell University, Ithaca, NY, USA
[2]Purdue University, West Lafayette, IN, USA

ABSTRACT

We demonstrate a hybrid oscillator system that combines the tunability of spin torque oscillators (STOs) with the exceptional quality factor (Q) of a high-overtone bulk acoustic resonator (HBAR) in a 2-chip system. The demonstrated magneto-acoustic oscillator (MAO) has a tuning range of 5% at 4 GHz with 175 kHz 3 dB linewidth. When compared to STOs we achieve a 200× reduction in linewidth, while retaining the original tuning range.

KEYWORDS

Spin torque oscillators, HBARs, tunable oscillators, narrow linewidth.

INTRODUCTION

Modern cellphone systems use a voltage controlled oscillator (VCO) which is phase-locked to a low-frequency crystal reference using a digital frequency divider. The VCO is then tuned to different frequency bands to down-convert the data from the carrier frequency. This consumes additional power for the circuits and needs more area for connecting to the off-chip crystal. A more elegant and integrated solution is a single oscillator which functions across several frequency bands whose output frequency can be changed to meet the requirements of the communication system. We can pick and choose a frequency of operation for efficient use of communication bandwidth with such an oscillator. This oscillator needs to have mass fabrication capability with a potential for CMOS co-fabrication to be produced cheaply and to provide an integrated solution. MEMS oscillators are poised to dominate the timing market due to comparable phase noise and frequency stability to the quartz-based oscillators and their capability for wafer level integration with CMOS [1]. One area where MEMS oscillators lag is in their frequency tuning ability. Typically, MEMS oscillators have a tuning range of only 100 ppm at gigahertz frequencies [2]. As a result, they cannot be used as a VCO for switching rapidly between different cellular bands.

Slonczewski [3] predicted that electron flow in a stack of magnetic materials carries angular momentum from one magnetic layer to another. This angular momentum exerts a torque on the magnetization of the magnetic layer and when the amplitude of the torque is sufficient to overcome the magnetic damping in the layer, the magnetization of the layer will oscillate. Shortly after this prediction, Kiselev *et al.* [4] were the first to perform direct measurements of microwave oscillations in nanostructures called spin torque oscillators. STOs consist of two conducting magnets called fixed and free magnets, which are separated by a spacer as shown in Figure 1. The magnetization of the free layer (or magnet) is susceptible to change by the angular momentum of the electrons impinging on it, while the magnetization of the fixed magnet is unaffected (or minimally affected) by the electron moment. Typically, the spacer used in these devices is of two types- conducting non-magnetic metals that have large spin relaxation lengths or insulating oxides like MgO. For the electron flow to apply sufficient torque to the magnet, a significant portion of the electron spins needs to be oriented along one direction. This orientation of electron spin in an STO is done by passing the electrons through the fixed layer magnet, where due to spin transfer torque, the electrons spins get reoriented along the direction of the magnetization of the fixed layer [5]. We use these spin-polarized electrons to apply torque to the magnetization of the free layer, causing its steady-state precession. Now in a spin torque oscillator, this magnetization precession can be read out electrically as a resistance change by the giant magnetoresistance effect or tunnel magnetoresistance effect [5].

$$f_0 = \frac{\gamma}{2\pi}\left[\left(H_{ap} + H_{an}\right)\left(H_{ap} + H_{an} + H_{de}^{ef}\right)\right] \qquad (1)$$

The frequency of oscillation f_o for a STO having a small precession angle is given by the Kittel formula shown in equation (1), where H_{ap} is the external applied magnetic field, H_{an} is the in-plane shape based anisotropy field, H_{de}^{ef} is the effective demagnetization field which depends on the orientation of the magnetization, and material property of the free layer and γ is gyromagnetic the ratio of the electron in free layer. The value of the gyromagnetic ratio divided by 2π for the typical materials used in spin torque oscillators is of the order of 28 GHz/T. Thus, a small change in the effective field seen by the free layer can cause a large change in frequency output. Nanofabricated STOs with nanometer thick free layers have oscillation frequency in 2-6 GHz range for typical materials and typical values of the effective fields [6]. The frequency of STO can be tuned over entire 2-6 GHz frequency range by changing the external applied magnetic field.

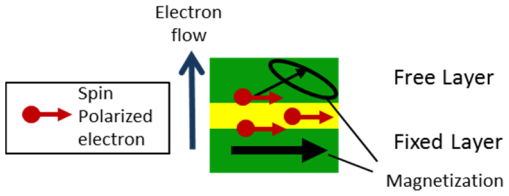

Figure 1: A Simplified cross-sectional stack of a spin torque oscillator showing magnetic layers in green separated by a non-magnetic spacer shown in yellow.

The frequency of the STO can also be tuned by changing the amplitude of spin transfer torque applied to the free layer magnet. This changes the trajectory of the magnetization precession thus changing the rate at which the resistance of the STO is being modulated. The amplitude of spin torque is proportional to the DC bias current applied to the STO. Thus, the oscillation frequency

can be tuned directly by changing the bias current. Typically, the tuning range of frequency due to the bias current is much smaller than the tuning range due to the applied field as the amplitude of the effective field due to the spin transfer torque is much smaller [5].

STOs have the potential for back-end CMOS integration and thus are the ideal solution to the needs of modern communication systems. STOs also have several other potential applications including being used as small form factor magnetic field sensor [7]. However, their applications are limited due to their large linewidths. We present a hybrid oscillator system called the magneto-acoustic oscillator, which leverages the tunability of the STO and the high quality factor of a multi-frequency MEMS resonator to overcome the limitations of standalone STOs. In MAO, the output of the STO is electrically filtered by the sharp frequency response of a two-port laterally-coupled HBAR [8], to generate frequency tunable narrow linewidth output. Such a hybrid system lets us retain the tunability of STOs while improving its linewidth over the entire tuning range by coupling them to multiple overtone modes of the HBAR.

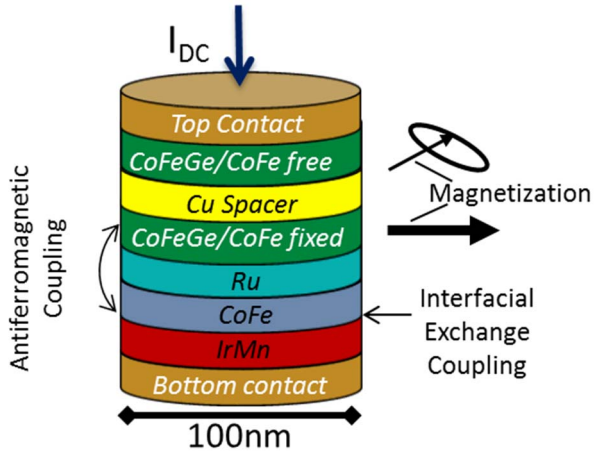

Figure 2: Schematic of spin valve nanopillar-based STO. Electrons due to I_{DC} apply spin torque to the magnetization of free layer causing its precession, which is read out as voltage oscillation.

FABRICATION

Spin valve nanopillar-based STO

Spin torque oscillator device uses CoFe/CoFeGe magnet as the free layer and fixed layer with Cu as a spacer. This configuration of the device, which has been demonstrated to have high magnetoresistance of about 6%, is called a spin valve nanopillar [9]. The overall device stack comprises of IrMn /CoFe /Ru /CoFeGe (30 Å) /CoFe (5 Å) /Cu (40 Å) /CoFe (5 Å) / CoFeGe (20 Å) as shown in Figure 2. In this device, IrMn, an antiferromagnet, due to interface exchange coupling with ferromagnetic CoFe layer pins the magnetization of the CoFe layer along a particular in-plane direction [9]. Thin Ru layer is then used to antiferromagnetically couple the pinned CoFe magnet to the fixed CoFeGe/CoFe magnet. The arrangement is used to cancel a dipole field between the free and the fixed layer and allows oscillation in absence of externally applied magnetic fields. CoFe (5 Å)/CoFeGe (20 Å) is the free layer magnet which is separated from reference layer using a 40 Å thick Cu spacer. The thickness of the antiferromagnet, pinning layer, the Ru spacer layer, the materials used in the seed and capping layers, which forms the top and bottom contacts, and the fabrication process flow are proprietary information and will not be disclosed in this paper. The spin torque oscillator has a circular shape with a diameter of 100 nm, which is ideal for measuring oscillations without an external bias magnetic field, making them attractive to implement them in complex standalone circuits.

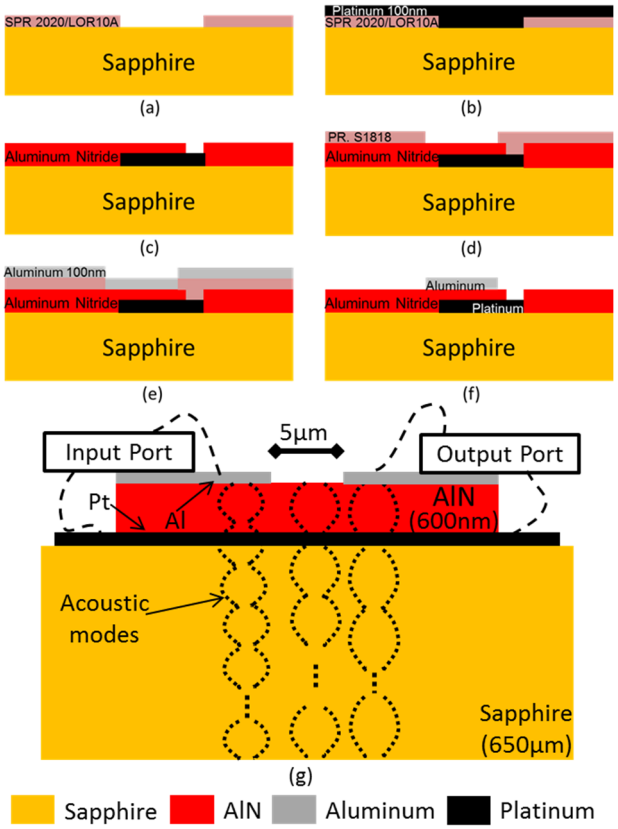

Figure 3: Fabrication process flow for laterally coupled two-port HBARs: (a) 650 µm thick double side polished C plane (0001) oriented sapphire substrates were used to for fabricating high quality factor two-port HBARs. (b) The bottom metal of 90 nm thick platinum with 10 nm of Ti seed layer was sputter deposited and patterned by liftoff. c) Piezoelectric AlN is deposited by reactive ion sputtering and is then etched using a photoresist mask in phosphoric acid heated to 160ºC to open a via for connecting to the bottom metal. (d) An S1818 photoresist mask is used for patterning the top electrode of aluminum. (e) 100 nm thick aluminum top metal is e-beam evaporated. (f) The top electrode is then patterned using lift-off with sonication. (g) Cross section of the HBAR shows input and output electrodes laterally spaced 5 µm from each other to have low transmission loss.

Two-port laterally-coupled HBAR

On a separate wafer, we fabricated two-port laterally-coupled HBAR devices on a 650 µm thick DSP sapphire substrates. Two-port HBAR devices are preferred over one port as they can be directly used as inline filters with low transmission loss in series with the STO to form the MAO. The fabrication process for HBAR devices and the device

cross section is shown in Figure 3. XRD measurements of the bottom Platinum electrode show that it has <111> orientation. This orientation is necessary to get a highly columnar C-axis oriented AlN piezoelectric layer. Rocking curve measurements on the AlN show an FWHM of 1.85º for the <200> peak confirming it is piezoelectric. AlN gets etched TMAH so CD-30, which is a soft developer that works efficiently with positive a photoresist such as S1818, was used for patterning AlN and the top electrode layers. Aluminum being light weight is the preferred material for the top electrode to reduce mass loading and for having a high quality factor of the HBAR. 600 nm thick AlN piezoelectric layer was used as the transducer to get multiple frequency resonances over the frequency range of 3-5 GHz. The input and output ports of the HBAR were spaced by 5 µm to get low transmission loss and high isolation over the entire frequency range of operation [8].

EXPERIMENTAL RESULTS

The STO, when biased above a DC threshold current of 200 µA, oscillates in the 3-4 GHz frequency range with peak output power of 5 pW. By increasing the bias current from 220 µA to 380 µA, the output frequency of the STO is changed from 4.05 GHz to 3.88 GHz as shown in Figure 4A. The mode of STO oscillation is in-plane hence, the oscillation frequency decreases with the increasing current as the magnetization precesses over a larger angle and a larger precession trajectory [6]. We measure the overall continuous tuning range of the STO to be 5% at 4 GHz oscillation frequency for a 170 µA change in the bias DC current.

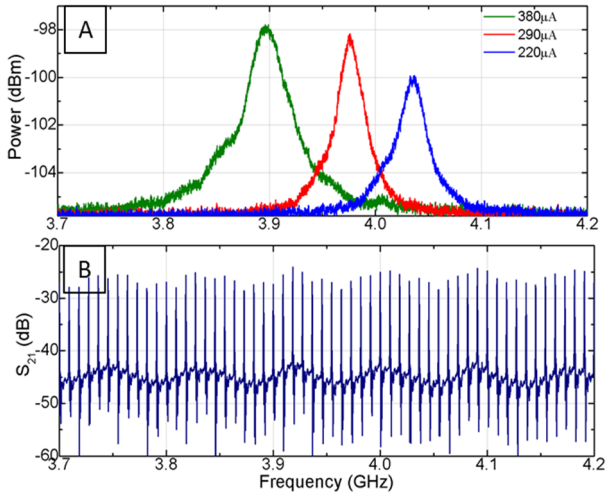

Figure 4: (A) Oscillation frequency of the STO, measured with Agilent E4440A spectrum analyzer, changes from 3.88 GHz to 4.05 GHz as the bias current is decreased by 160 µA. The measurements were performed without an external bias magnetic field (B) Measured transmission response of the HBAR in dB shows multiple resonances corresponding to different thickness expansion modes of the sapphire substrate. The frequency spacing between resonances is 9.1 MHz.

Two port transmission response of the HBAR measured using an Agilent N5230A parametric network analyzer is shown in Figure 4B. The HBAR has high quality factor resonances over the entire frequency range of 3-5 GHz with Q greater than 22,000 and transmission loss less than -25 dB at the resonance peak. This transmission loss is dependent on the lateral spacing between the input and the output ports. It is possible to further reduce the transmission loss by reducing the lateral spacing between the two ports [8]. The quality factors measured using the Q-Circle method [10] corresponds to the highest f-Q product of 1.01×10^{14} Hz for the resonance frequency of 3.982 GHz. The stop band rejection of the HBAR filter was measured to be greater than 18 dB for all the resonances over the frequency range of 3-5 GHz. The spacing between the resonances was measured to 9.1 MHz, which corresponds to the sapphire wafer thickness of 650 µm.

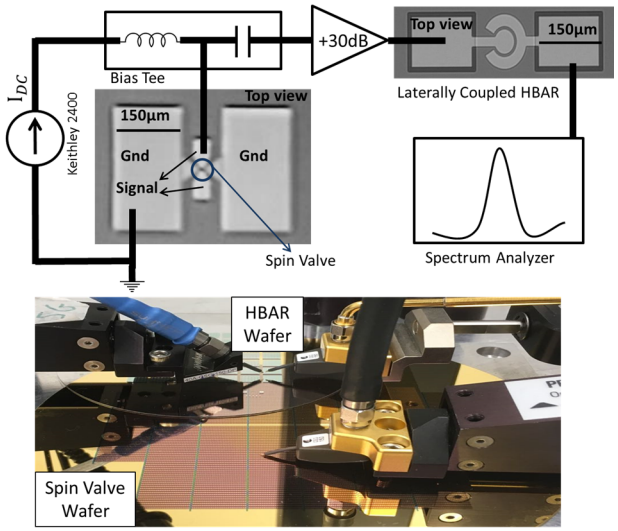

Figure 5: (A) Measurement setup for the magneto-acoustic oscillator shows the output of the STO is filtered by the high Q HBAR to get narrow linewidth oscillator. The output frequency of the MAO is set by the oscillation frequency of the spin valve (STO) which is tuned by changing I_{DC}. (B) Picture of the measurement setup for the MAO.

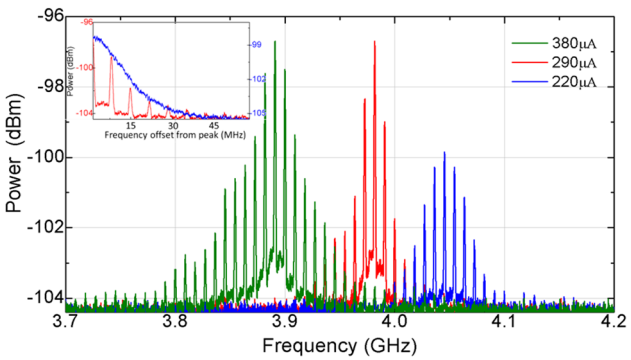

Figure 6: Output of magneto-acoustic oscillator for different bias currents shows tunable operation with narrow linewidth at the frequency corresponding to the oscillation peak. The inset shows the enhanced linewidth of the MAO in red of 175 kHz plotted from the center peak compared to the direct output of the STO in blue, which has the linewidth of 35.2MHz for I_{DC} of 290 µA.

In the magneto-acoustic oscillator, the STO acts as a tunable frequency generator whose output signal is amplified and fed to the two port HBAR. The HBAR acts

as a multi-frequency inline bandpass filter that allows signal transmission only at frequencies corresponding to its resonances. The output signal from STO is thus shaped by the transmission response of the HBAR and the linewidth of the MAO is given by the bandwidth of the transmission peak of the HBAR resonance. The measurement setup for the MAO is shown in Figure 5. We use an amplifier with 30 dB gain to compensate for the -25 dB transmission loss in the HBAR. The amplifier being used in an open loop configuration doesn't contribute any frequency noise to the linewidth of the magneto-acoustic oscillator. Figure 5B shows the picture of the measurement setup of the MAO where we use RF probes and high-frequency SMA cables to electrically connect the STO to the HBAR both of which are fabricated on separate wafers.

Changing the DC bias current of the STO when connected in the MAO configuration from 220 μA to 380 μA tunes the output of the MAO from 4.05 GHz to 3.88 GHz as shown in Figure 6. As the STO frequency, changes the oscillation output traverses a path across the HBAR transmission. As the linewidth of STO is 35.2 MHz while the frequency spacing between the HBAR resonances is 9.1 MHz we see multiple peaks for one bias DC current at the output of the MAO. The highest power peak observed at the output of the MAO corresponds to the HBAR resonance frequency closest to the peak of the STO output. By using a thinner substrate for fabricating the laterally coupled HBAR, we can increase the spacing between the HBAR resonances and thus get a cleaner output for the MAO with lesser number of peaks for a given linewidth of the STO. Another option is to use an STO with narrower linewidth [6]. The MAO output has a linewidth of 175 kHz at 3.982 GHz corresponding to the high quality factor of the HBAR resonance. This is a 200× reduction from the original linewidth of 35.2 MHz for a standalone STO for an input DC bias current of 290 μA. Similar improvement in linewidth of STO output is seen across the entire frequency tuning range when it is implemented as part of the magneto-acoustic oscillator. Table 1 shows the comparison between a high-performance MEMS oscillator, a spin torque oscillator, and the magneto-acoustic oscillator where for the MAO, we get narrow linewidth from the HBAR and large frequency tuning capability of the STO.

Table 1: Magneto-Acoustic oscillator performance compared to MEMS Oscillators and STOs

Oscillator Type	Linewidth	Tuning range
MEMS oscillator [1]	>1Hz	~0.4%
STO	>30MHz	5%
MAO –this work	175kHz	5%

CONCLUSION

In summary, we present the first magneto-acoustic oscillator, which leverages the high quality factor of the HBAR and the tunability of STO to give a narrow linewidth oscillator with a linewidth of 175 kHz and frequency tuning range of 5% at 4 GHz. The linewidth and the frequency stability of the magneto-acoustic oscillator can be further improved by implementing it in a feedback system. In such a configuration, the output of the open loop MAO which is frequency filtered by the high quality factor of the HBAR would be used to injection lock the spin torque oscillator. The HBAR in a feedback system with the STO forms a mechanical delay line with a large time constant corresponding to its high quality factor. This mechanical delay line will further improve the linewidth of the magneto-acoustic oscillator in a closed loop feedback system.

ACKNOWLEDGEMENTS

The authors would like to thank the SRC and the Cornell Center for Material Research with funding from NSF MRSEC program (DMR- 1120296). This work was performed in part at the Cornell NanoScale Facility, a member of the NNCI, which is supported by the NSF (Grant ECCS-15420819). We also would like to thank Dr. Patrick Braganca of HGST for fabricating STO devices and for many insightful discussions.

REFERENCES

[1] R. Ruby *et al.*, "Positioning FBAR technology in the frequency and timing domain," *IEEE Trans. Ultrason. Ferroelectr. Freq. Control*, vol. 59, no. 3, pp. 334–345, 2012.

[2] J. T. M. van Beek and R. Puers, "A review of MEMS oscillators for frequency reference and timing applications," *J. Micromechanics Microengineering*, vol. 22, no. 1, p. 13001, 2012.

[3] J. C. Slonczewski, "Current-driven excitation of magnetic multilayers," *J. Magn. Magn. Mater.*, vol. 159, no. 1, pp. L1–L7, 1996.

[4] S. I. Kiselev *et al.*, "Microwave oscillations of a nanomagnet driven by a spin-polarized current," *Nature*, vol. 425, no. 6956, pp. 380–383, 2003.

[5] D. C. Ralph and M. D. Stiles, "Spin transfer torques," *J. Magn. Magn. Mater.*, vol. 320, no. 7, pp. 1190–1216, 2008.

[6] T. Chen *et al.*, "Spin-Torque and Spin-Hall Nano-Oscillators," *Proc. IEEE*, vol. 104, no. 10, pp. 1919–1945, 2016.

[7] P. M. Braganca, B. A. Gurney, B. A. Wilson, J. A. Katine, S. Maat, and J. R. Childress, "Nanoscale magnetic field detection using a spin torque oscillator," *Nanotechnology*, vol. 21, no. 23, p. 235202, 2010.

[8] A. Reinhardt *et al.*, "Ultra-high Q.f product laterally-coupled AlN/silicon and AlN/sapphire High Overtone Bulk Acoustic wave Resonators," in *2013 IEEE International Ultrasonics Symposium (IUS)*, 2013, pp. 1922–1925.

[9] S. Maat, M. J. Carey, and J. R. Childress, "Current perpendicular to the plane spin-valves with CoFeGe magnetic layers," *Appl. Phys. Lett.*, vol. 93, no. 14, p. 143505, 2008.

[10] D. A. Feld, R. Parker, R. Ruby, P. Bradley, and D. Shim, "After 60 years: A new formula for computing quality factor is warranted," in *2008 IEEE Ultrasonics Symposium*, 2008, no. 6, pp. 431–436.

CONTACT

*T. A. Gosavi; tag75@cornell.edu